THE ASTROPHYSICAL JOURNAL, 296:576–592, 1985 September 15

ON THE OUTER ATMOSPHERES OF HYBRID STARS

L. HARTMANN,[1,2] C. JORDAN,[2,3] A. BROWN,[2,4] AND A. K. DUPREE[1,2]

Received 1984 October 3; accepted 1985 March 18

ABSTRACT

We discuss a variety of ultraviolet observations of four hybrid atmosphere stars, objects which exhibit both cold winds and high-temperature (transition-region) emission. New short-wavelength ($\lambda\lambda$1200–2000) exposures made with the *International Ultraviolet Explorer* satellite (*IUE*) confirm that the K3 II stars ι Aur and θ Her are hybrid stars. In addition, γ Aql (K3 II) is found to be another hybrid object. It is shown that long exposures with the *IUE* satellite are necessary to place meaningful constraints on high-temperature emission lines.

High-dispersion observations of the hybrid star α TrA (K4 II) confirm the large broadening of the C IV emission lines previously reported and provide a measurement of the electron density from the C II density sensitive lines. The emission-line fluxes are used to derive emission measure distributions, and assuming the derived density is characteristic of all the hybrid stars, we explore some simple atmospheric models. The material at temperatures $\sim 2 \times 10^5$ K in these envelopes probably has a scale height that is an appreciable fraction of the stellar radius. The Si III] and C III] line widths are probably dominated by turbulent broadening rather than expansion, and such turbulent motions may dominate thermal gas pressure in determining the extension of the hot outer envelope. We cannot tell if this envelope is expanding.

Monitoring of the Mg II resonance line profiles demonstrates that the high-velocity circumstellar shell absorption in λ Aql, θ Her, and α TrA varies on time scales of a year. There is little evidence for concurrent changes in emission-line fluxes, suggesting that the profile changes are not chromospheric in nature but are produced by variability in the distant wind properties.

Very deep exposures of the Mg II emission lines in α TrA show that wind absorption is visible at velocities up to 180 km s^{-1} relative to the photosphere. These observations suggest that high-velocity mass loss is more common than previously thought.

Subject headings: stars: chromospheres — stars: coronae — stars: late-type — stars: mass loss — ultraviolet: spectra

I. INTRODUCTION

The hybrid atmosphere stars are objects that exhibit emission in lines formed around 10^5 K (e.g., N V, C IV, Si IV), as well as winds with temperatures $\lesssim 10^4$ K (Hartmann, Dupree, and Raymond 1980). The study of hybrid stars is of importance to theories of stellar mass loss. Previous observations suggested that some form of solar-type activity may be responsible for producing the low-temperature, expanding circumstellar shells (Hartmann and MacGregor 1980). The large widths of the Doppler-broadened transition region lines led Hartmann, Dupree, and Raymond (1981) to suggest that the winds from hybrid stars may be at temperatures $> 10^4$ K, so that further studies might produce a better understanding of the change from high-temperature, coronal winds to low-temperature flows. In addition, stars with high-velocity circumstellar shells, of which the hybrids are an example, commonly exhibit variable winds (cf. Reimers 1977). Thus, continuing observations should provide additional insight into the mechanisms of mass loss.

The location of hybrid stars in the H-R diagram also plays an important role in understanding the way in which hot outer envelopes are produced. Simon, Linsky, and Stencel (1982) attempted to determine the location of a division between stars with and without high-temperature outer atmospheres. They found a dividing line which is fairly close to the line proposed by Linsky and Haisch (1979). However, the K4 II hybrid atmosphere star α TrA (Hartmann, Dupree, and Raymond 1981) does not agree with this dividing line, and Reimers (1982) has suggested that two of the cool atmosphere stars of Simon, Linsky, and Stencel (1982), ι Aur (K3 II) and θ Her (K3 II), also exhibit high-temperature emission, and so are inconsistent with this simple division.

In order to investigate some of these problems further, we have obtained deep exposures with the *IUE* satellite in order to search for high-temperature emission from stars with cool winds. We confirm that ι Aur and θ Her are hybrid stars and have discovered an additional hybrid object, γ Aql. Since all of these stars are relatively bright, and the exposure times required for the detection of the high-temperature emission are long, it appears quite possible that many more hybrid stars exist with transition region emission below the sensitivity limit of *IUE*. The possibility of evolutionary effects producing lower carbon abundances further complicates the interpretation of C IV upper limits. The observations are discussed in § II.

In § III we analyze the emission-line fluxes to establish the emission measure distribution and, as far as possible, the electron density. The extent to which the data, including line widths, can or cannot be satisfied by simple, spherically symmetric, hydrostatic and expanding models in a self-consistent manner places constraints on the atmospheric structure. The effects of "turbulent" support are also considered briefly.

In § IV we report the discovery of variable, high-velocity Mg II circumstellar absorption in γ Aql, θ Her, and α TrA. Very long exposures of α TrA show that cool material is being accel-

[1] Harvard-Smithsonian Center for Astrophysics.
[2] Guest Observer, *International Ultraviolet Explorer*.
[3] Department of Theoretical Physics, Oxford University.
[4] Joint Institute for Laboratory Astrophysics.

erated to velocities of at least 180 km s^{-1}. The implications of these observations are considered in the final section of the paper.

II. OBSERVATIONS

Ultraviolet spectra of ι Aur, γ Aql, and θ Her were obtained using the *International Ultraviolet Explorer* satellite. Details of the instrument and performance may be found in Boggess *et al.* (1978). Observations were made in both the short-wavelength (1150–1950 Å), low-dispersion mode, and in the long-wavelength (2000–3200 Å), high-resolution mode. In addition, high-dispersion, short-wavelength and long-wavelength spectra of the bright hybrid star α TrA were obtained. All exposures were made through the large apertures ($\sim 10'' \times 20''$). Exposure times and dates are given in Table 1.

a) Short-Wavelength Spectra

Sample low-dispersion spectra of the program stars are shown in Figure 1, and the line fluxes are listed in Table 2. The absolute calibration was taken from Bohlin and Holm (1980).

There is little evidence for variability in the emission lines, so we generally have adopted the measurements from our longest exposures (SWP 17719, 17721, and 17722). The O I and Si II lines are saturated on the deep exposures, so the fluxes for these lines are taken from the earlier, more weakly exposed spectra (SWP 15474, 16462, 16363, and 16548). A : symbol has been adopted to indicate an uncertain flux measurement.

The identification of lines at low-dispersion can be difficult, given the ~ 6 Å resolution for the SWP exposures. In addition, exposures in the large apertures introduce the possibility of substantial wavelength offsets. Harvel, Turnrose, and Bohlin (1979) have shown that new procedures for large-aperture SWP exposures yield typical offset errors ~ 2.2 Å and scale errors ~ 0.7 Å. We have used relatively strong emission lines of the low-temperature ions S I $\lambda\lambda$1296, 1900, 1914; O I λ1355.6; C I λ1657; and Si II $\lambda\lambda$1808, 1817 to establish the wavelength offsets of our spectra. High-dispersion spectra of late-type stars with and without high-temperature emission indicate the correctness of these identifications (cf. Hartmann, Dupree, and Raymond 1981; Carpenter and Wing 1979; Brown and Jordan 1981). The wavelength offsets derived from the low-temperature lines, as well as the dispersion in offsets, are consistent with the results of Harvel, Turnrose, and Bohlin (1979).

TABLE 1

SUMMARY OF EXPOSURES

Star	Image	Date (y/d)	t_{exp} (minutes)
ι Aur	LWR 11959	1981/315	25
	LWR 12701	1982/61	25
	SWP 15474	1981/315	90[a]
	SWP 16458	1982/60	210[a]
	SWP 17719	1982/230	465[a]
γ Aql	LWR 11957	1981/315	20
	LWR 12700	1982/60	30
	SWP 15473	1981/315	60[a]
	SWP 16462	1982/61	185[a]
	SWP 17721	1982/231	510[a]
θ Her	LWR 12699	1982/60	80
	LWR 13334	1982/148	50
	SWP 16463	1982/148	180[a]
	SWP 17722	1982/232	385[a]
α TrA	LWR 7739	1980/134	30
	LWR 9883	1981/40	30
	LWR 11972	1981/318	10
	LWR 13332	1982/148	10
	LWR 13980	1982/231	240
	LWR 13981	1982/231	240
	LWR 13982	1982/231	10
	SWP 8986	1980/134	540
	SWP 8987	1980/134	60[a]
	SWP 11272	1981/40	70[a]
	SWP 15494	1981/317	1135

NOTE.—All exposures were taken through the large apertures.

[a] Low-dispersion spectrum.

TABLE 2

LOW-DISPERSION EMISSION-LINE FLUXES AT EARTH[a]

λ(Å)	Ion	ι Aur	γ Aql	θ Her	α TrA
1240.....	N V	≤0.65[b]	≤0.3[b]	≤0.6[b]	2.4
1550.....	C IV	0.8	1.0	0.6	4.8
1400.....	Si IV	1.0:[c]	0.5:[c]	0.5:[c]	2.7
1640.....	He II + O I	0.8	1.6	0.8	2.6
1909.....	C III	0.3:[c]	0.5:[c]	0.3:[c]	2.8
1892.....	Si III	0.4:[c]	0.6:[c]	0.6:[c]	2.8
1335.....	C II	0.45	0.9	0.3	2.9
1808.....	Si II	0.8	1.4	0.9	13.2[d]
1817.....	Si II + S I	2.1	3.5	2.1	
1303.....	O I	15	26	9	...
1660.....	C I	1.2	2.3	0.6	4.3
1296.....	S I	4.3	6.0	2.5	...
1475.....	S I	0.8	1.2	0.7	...
1900.....	S I	0.4:[c]	0.6:[c]	0.3:[c]	1.9
1914.....	S I	0.2:[c]	0.2:[c]	0.2:[c]	1.3

[a] Fluxes in units of 10^{-13} ergs cm^{-2} s^{-1}.

[b] The ≤ symbol denotes an upper limit to possible detected emission near N V.

[c] The : symbol denotes an uncertain flux measurement.

[d] Sum of emission line fluxes of the 1808 and 1817 Å features.

We find emission features in the long exposures that are consistent with the wavelengths of the high temperature lines C IV λ1549, Si IV λ1394, C III] λ1909, Si III] λ1893, and C II λ1335. For example, the high-temperature lines in SWP 17721 for γ Aql are displaced by -0.2 ± 1.0 Å relative to the low-temperature lines. There is some indication of emission consistent with the wavelengths of N V λ1240 and Si IV λ1403 in the long exposures.

Ayres, Moos, and Linsky (1981) pointed out that fluorescence in CO bands can produce emission which can be confused with C II and C IV emission. However, this fluorescence in α Boo produces features at 1380 Å and 1600 Å which are stronger than other fluorescent features near 1340 Å and 1545 Å. This is not observed in our long exposures, and the difference is particularly striking for C IV, which is very much stronger in our hybrid stars than the 1600 Å emission.

Our identification of high-temperature emission lines in the program stars is based on the following points:

1. Si III] and C III] have been unambiguously detected in all three stars. Fluxes are somewhat uncertain because of crowding with the S I lines at 1900 and 1914 Å and the continuum contribution, but there is no problem in demonstrating the presence of Si III and C III with the 6 Å resolution of *IUE* (compare Fig. 1 with Fig. 2 of Ayres, Moos, and Linsky).

2. Si IV emission has been detected in ι Aur and γ Aql. N V may also have been detected in these objects.

3. There is considerably more emission near C II and C IV relative to presumed fluorescent CO emission in the program stars than is observed in cool atmosphere stars like α Boo.

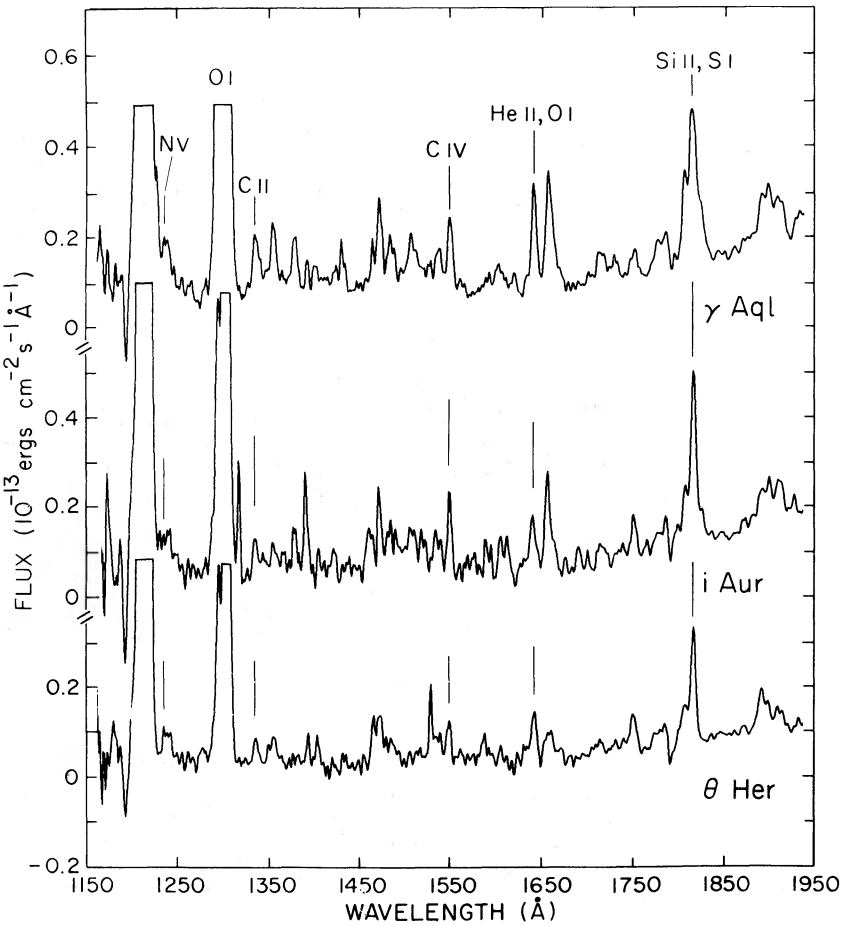

FIG. 1.—Low-dispersion, short-wavelength spectra of three hybrid stars. The long exposures show the presence of high-temperature ions (e.g., C IV, N V).

4. As described below, flux ratios of the presumed high-temperature emission lines in the program stars are similar to those observed in the known hybrid star α TrA. Thus, we conclude that ι Aur, γ Aql, and θ Her are hybrid stars, exhibiting emission from gas at temperatures in excess of 2×10^4 K.

There are unidentified features in the spectrum. Lines at 1378.7 ± 1 Å and 1607.3 ± 1 Å are similar in wavelength to those that appear in cool giants. Although coincidences with lines from neutral atoms, singly charged ions, and the CO fourth positive system can be found, there is no systematic behavior which allows definite identifications at low resolution.

The photowrite of the spectrum of ι Aur shows the presence of further emission to the short wavelength side of the S I 1296 Å blend. This may be due to Fe II excited by H Lyα—a mechanism suggested by Brown, Jordan, and Wilson (1979) and recently confirmed in the spectra of the M supergiant β Gru (Johansson and Jordan 1984). The weak unidentified features will be difficult to observe at high resolution even with two consecutive *IUE* shifts, and their definite identifications may have to await the Space Telescope.

b) *High-Dispersion SWP Exposure of α TrA*

A 14 hr exposure in the high-dispersion mode of the short-wavelength region in α TrA was obtained, providing better measurements of the widths of the high-temperature lines than given by Hartmann, Dupree, and Raymond (1981). The spectrum confirms the presence of N V emission.

The Lyα profile is exhibited in Figure 2, corrected for the echelle blaze function following Ake (1981). After blaze correction, the line profiles measured from two independent orders agree quite well in the region of overlap. The observed profile and asymmetry results from a combination of interstellar absorption, absorption in the expanding circumstellar shell, and intrinsic asymmetry of the emission produced in an expanding chromosphere.

The absolute flux calibration for this line is uncertain. We have adopted a ratio of 150 as the factor between the low-dispersion and high-dispersion sensitivity from extrapolating the results of Cassatella, Ponz, and Selvelli (1981) for emission-line spectra, but this value might be in error by 50% or so. Cassatella *et al.* derive a sensitivity ratio ~200 for continuous spectra, but it seems likely that this ratio is increased by background subtraction problems not present in our emission-line spectrum.

Figure 3 displays the O I line profiles, which are also asymmetric. The peaks of the O I lines are saturated, and the 1302 Å line is marred by a camera reseau. The 1304.81 Å and 1305.89 Å lines in SWP 15494 show clear evidence for absorption features on the short-wavelength side. This structure is real, as it is also visible in the repeated line spectra in the adjacent echelle order. These absorption components are not obviously present in SWP 8986. It is not clear whether this represents a real

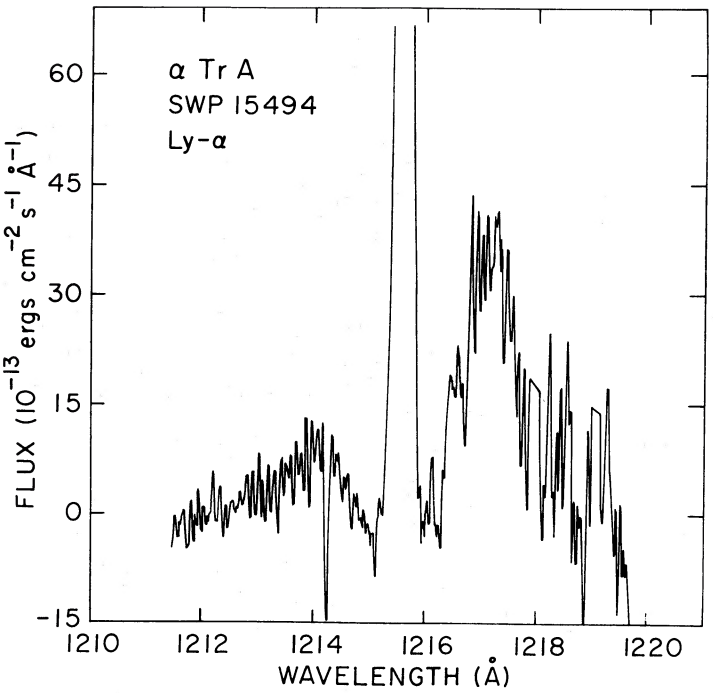

FIG. 2.—Lyα profile of α TrA. The central part of the profile is masked by geocoronal emission. The profile longward of about 1218 Å is uncertain; two radiation noise spikes near 1218 and 1219 Å have been truncated.

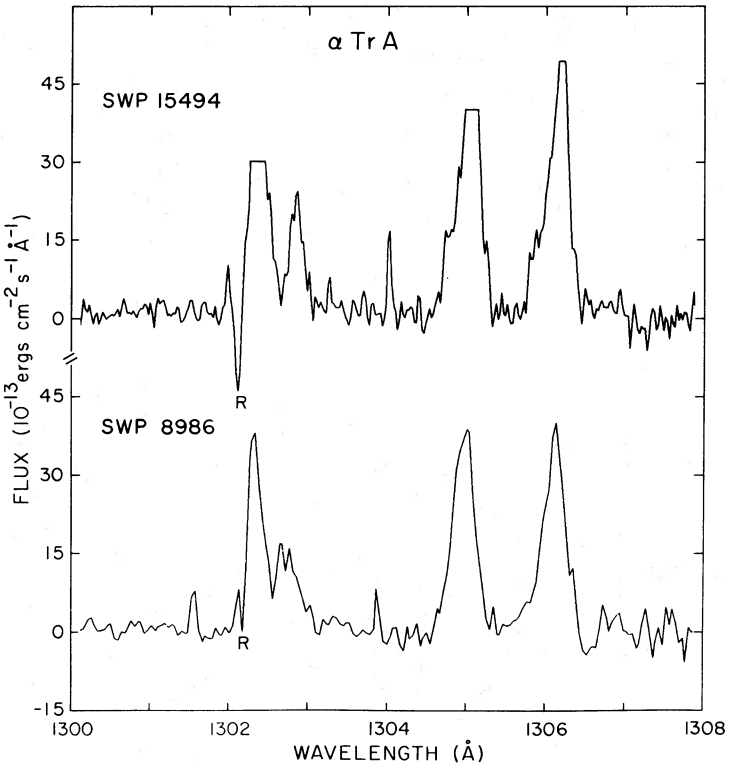

FIG. 3.—O I line profiles in α TrA. The peaks of the lines are saturated, and R marks a camera reseau.

TABLE 3

OBSERVED HIGH-DISPERSION FLUXES IN α TRIANGULI AUSTRALIS

Spectrum	Atom	λ (Å)	f_0(ergs cm^{-2} s^{-1})
SWP 8986	Si III]	1892	2.8 (−13)[a]
	C III]	1909	2.6 (−13)
	S I	1900	2.0 (−13)
	S I	1914	1.3 (−13)
SWP 15494	Lyα	1215	7.7 (−13)
	O I	1641.7	2.3 (−13)
	O I	1304.9	2.2 (−12)
	C I	1993.6	2.3 (−13)
	O I	1657.4	1.1 (−13)
LWR 13980+13981	C II]	2325	3.5 (−12)
	Al II]	2670	1.5 (−12)

[a] Number in parentheses indicates power of 10.

variation, since data processing changes in the interval between these two spectra mean that the SWP 15494 spectrum has twice as many samples, and thus improved resolution. Since the structure of the lines at 1305.9 Å and 1306.2 Å is similar, absorption by S I, which pumps the S I emission seen near 1296 Å and 1302.8 Å, seems unlikely to be its sole cause (cf. Brown and Jordan 1981; Hartmann, Dupree, and Raymond 1981). Absorption out of the excited states of the O I ground triplet is not observed in the interstellar medium, and we conclude that the origin of the low velocity absorption is either chromospheric or at least in the vicinity of the star. A chromospheric self-reversal is expected, given the estimated opacity in the O I lines. Similarly, an asymmetric, self-reversed profile of chromospheric origin is expected for the Mg II lines in addition to interstellar absorption (see below).

The emission around 1640 Å detected at low resolution is observed to have two components in the high-resolution spectrum—a broad, weak emission at the wavelengths of the He II Baα blend, and a narrow, strong line at 1641.3 Å, which is due to O I] pumped by the O I resonance lines (Brown, Ferraz, and Jordan 1981). The observed He II contribution is similar to that assumed by Hartmann, Dupree, and Raymond (1981) in deriving an upper limit to the high-temperature emission measure, and is discussed further below. Line fluxes for selected important and unsaturated lines are presented in Table 3. A value of 100 for the ratio of low-dispersion to high-dispersion sensitivity was adopted, in rough agreement with the results of Cassatella, Ponz, and Selvelli (1981).

TABLE 4

EMISSION-LINE WIDTHS IN α TRIANGULI AUSTRALIS

Spectrum	Line	FWHM[a]
SWP 8986	C III	99
	Si III	76
	C IV	150–200
	Si II λ1808	75
	C I λ1994	50
SWP 15494	C IV	150–200
	N V	120–160
	O I λ1355	≤30
	O I λ1641.3	≤30
	S I λ1900	≤40
	S I λ1914	≤30
	C I λ1994	40
LWR 13980	C II λ2325	56
LWR 13981	C II λ2325	51

[a] Full width at half-maximum intensity, in km s^{-1}.

TABLE 5

Mg II *h* LINE FLUXES

Star	Spectrum(LWR)	f_0[a]
γ Aql	11957	1.27
	12700	1.42
	13984	1.52
ι Aur	11959	1.03
	12701	0.97
	13979	1.04
θ Her	12699	0.58
	13978	0.53
α TrA	13982	3.6

[a] Observed fluxes at Earth in units of 10^{-11} ergs cm^{-2} s^{-1}.

The line widths and velocities from the high-dispersion spectra are given in Table 4. The results agree reasonably well with the values presented by Hartmann, Dupree, and Raymond (1981). Unfortunately, the low signal-to-noise values for the emission in lines like C IV preclude an accurate determination of the radial velocities, as performed for other objects by Ayres *et al.* (1983). The radial velocities of the other emission lines are consistent with each other within our measurement errors of about 10 km s^{-1}. The low signal-to-noise values of our spectra, the presence of radiation noise spikes, and high backgrounds, preclude more accurate measurements.

c) *Long-Wavelength, High-Dispersion Spectra*

The Mg II emission line fluxes derived from LWR high-dispersion exposures are presented in Table 5. Echelle blaze corrections and sensitivity high-dispersion calibrations were performed as in Hartmann, Dupree, and Raymond (1982). Fluxes are listed for the *h* line only, because the exposure times required to study the absorption components were generally long enough to saturate the *k* line peak.

We list in Table 6 the velocities of absorption components in Mg II *k* and *h* for ι Aur, θ Her, and γ Aql. Velocities relative to each star were determined by reference to photospheric features. The measurements of high-velocity absorption refer to the minimum intensity points and do not correspond to the highest velocities at which absorption effects are seen. Variations in the velocities of the minimum intensity points are small, except in the case of α TrA (see below). All of the program stars exhibit the "double" absorption profiles suggested by Reimers (1982) to be characteristic of hybrid stars.

No evidence for Mg II variability in ι Aur is noted (Fig. 4). Our observations of θ Her indicate much more short-wavelength emission compared with Reimers's (1982) spectra, even though the "velocities" of the two absorption components are quite close to the values of −100 and −13 km s^{-1} found by Reimers. Our interpretation is that high-velocity wind present

TABLE 6

Mg II ABSORPTION VELOCITIES

Star	Spectrum (LWR)	ΔV_1 (km s^{-1})	ΔV_2 (km s^{-1})
γ Aql	12700	−29	−75
ι Aur	12701	−8	−72
θ Her	12699	−5	−91
	13978	−6	−74

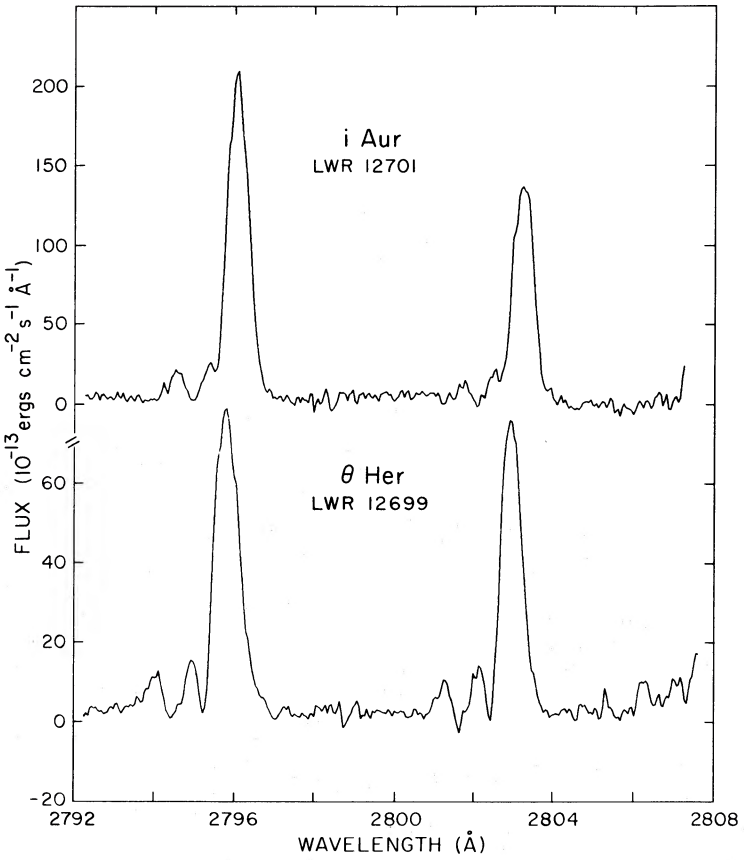

FIG. 4.—Mg II resonance line profiles in ι Aur and θ Her. The peak emission in the k lines is slightly saturated.

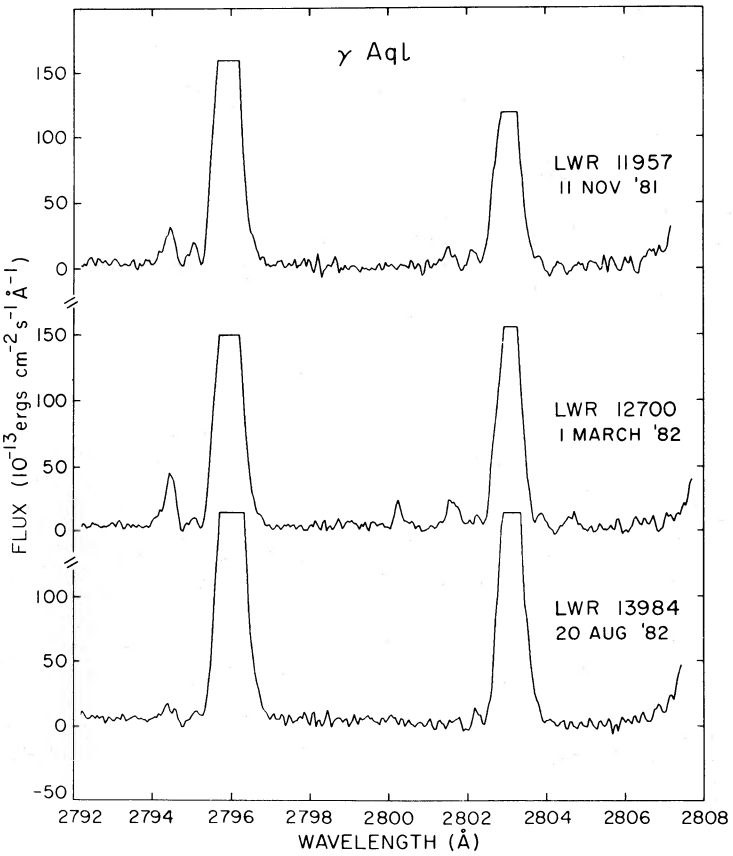

II resonance line profiles in γ Aql. The short-wavelength emission is variable, probably due to variations in the high-velocity circumstellar

FIG. 5.—Mg absorption.

at the time of Reimer's observations scattered out the underlying short-wavelength chromospheric emission, and that the optical depth of high-velocity material was much less during our observation. We rule out chromospheric emission changes, because we can detect no similar effect on the long-wavelength side of the line profiles. Similar changes in the short-wavelength emission in γ Aql may be occurring (Fig. 5), although the variations are near the threshold for detection. It is misleading to cite a single velocity characterizing the minimum intensity in the line profile as the "wind velocity," as absorption is clearly present over a significant velocity range.

Figure 6 shows the time variability of the Mg II line profiles in α TrA. In 1980 May the profiles were essentially identical to a spectrum taken 2 months earlier (Hartmann, Dupree, and Raymond 1981). However, by 1981 the short-wavelength emission had decreased substantially. The spectra indicate that a small amount of residual short-wavelength emission in the *k* line had disappeared in 1982.

In 1982 we obtained two long, high-dispersion exposures in order to detect the density-sensitive C II lines at 2325 Å (see § III*c*). Fortuitously, these spectra enabled us to observe the true extent of the high-velocity absorption (Fig. 7). With these long exposures, the Mg II emission peaks are saturated, but the high-velocity absorption in the faint line wings becomes detectable. The absorption extends out to about -180 km s^{-1} relative to the star. The absorption has the form of a trough, which suggests that large differential motions are present in this cool wind that are highly supersonic, perhaps indicating continuing acceleration of the cold wind.

In all of the above cases, the changes in total line fluxes are small or negligible. This indicates that the profile changes are due to variations in the high-velocity wind, rather than in the chromosphere.

Drake, Brown, and Linsky (1984) have recently suggested that the low-velocity absorption component in the Mg II lines of stars with "double" absorption may be interstellar in origin. Whereas an interstellar component of Mg II is expected for stars of this distance and Galactic position, so is an intrinsic self-reversal, given the estimated line opacity. Observations of the Ca II resonance lines (Reimers 1982) show self-reversals

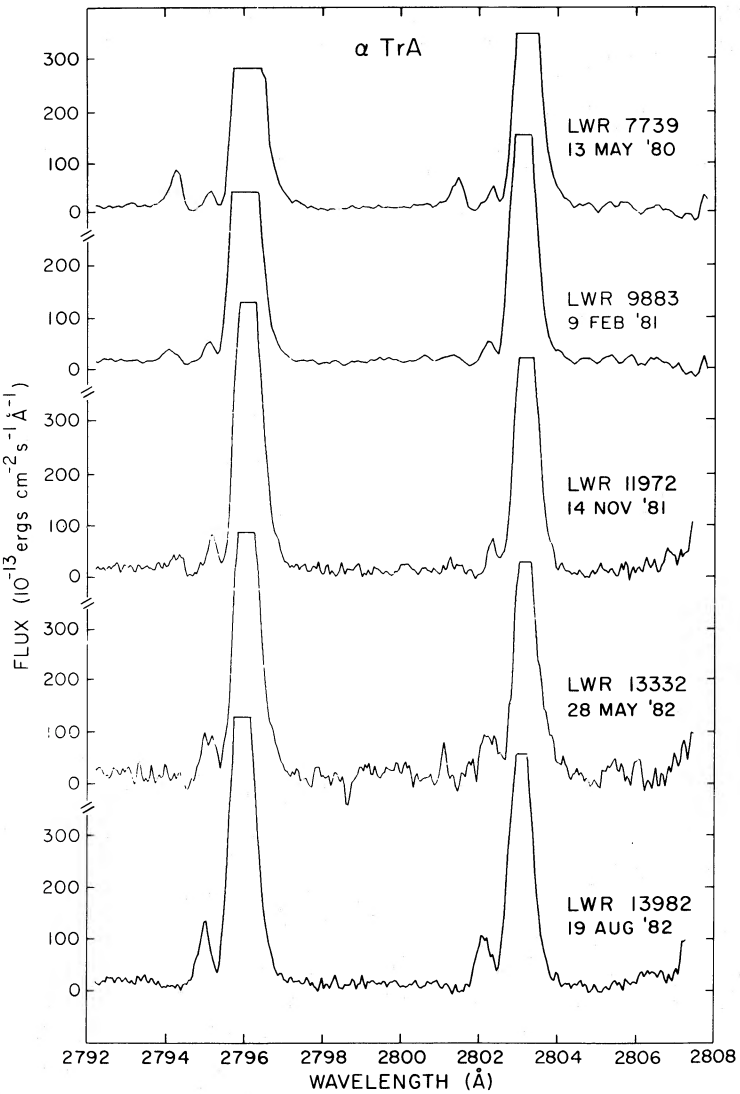

FIG. 6.—Time sequence of Mg II line profiles in α TrA, showing the disappearance of short-wavelength emission

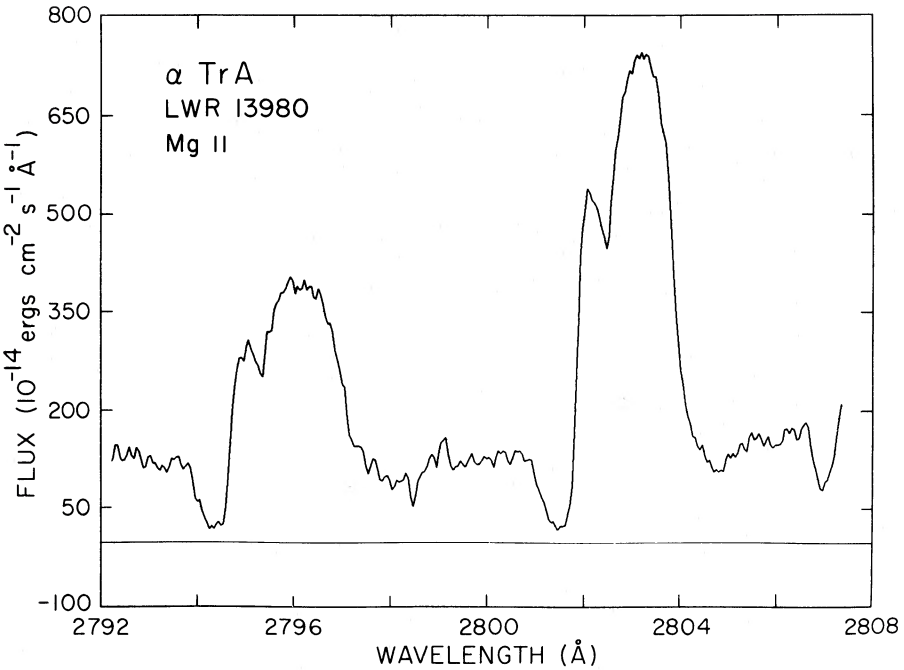

FIG. 7.—Heavily exposed Mg II spectrum in α TrA. The line emission is overexposed by a factor of about 20 (see Fig. 6). Fluxes above 2×10^{-12} ergs s^{-1} cm^{-2} Å^{-1} for the *k* line and 3.5×10^{-12} ergs s^{-1} cm^{-2} Å^{-1} for the *h* line are saturated or on extrapolated portions of the intensity transfer function. Very high velocity circumstellar absorption is seen to be present.

that are largely chromospheric and not interstellar, given the large velocity width of the absorption, and it is reasonable to suppose that the Mg II lines exhibit similar behavior. Calculations of the line profiles from chromospheric models will be required to determine the relative contributions of these two processes, but the O I profiles show clearly the presence of low-velocity chromospheric matter.

As discussed by Stencel *et al.* (1981), the C II lines near 2325 Å can be used to determine electron densities in the range (10^7–10^9) cm^{-3}. Accordingly, two 4 hr LWR exposures of α TrA were taken in order to obtain reasonable detections of these lines. One of the spectra is shown in Figure 8, and the line fluxes and ratios are summarized in Table 7. The electron density derived from these lines is discussed in § IV. The long-wavelength spectra also allow the flux in the Al II] line at 2690 Å to be measured.

d) Comparison of Results with Previous Observations

We find generally fair agreement between the line fluxes derived by us and those of Simon, Linsky, and Stencel (1982) for ι Aur and γ Aql, particularly considering the low exposure levels involved. Our C IV fluxes for ι Aur and γ Aql are 2 and 2.5 times the 1 σ upper limits given by Simon, Linsky, and Stencel (1982) for these stars. C IV is not apparent on our earliest, short SWP exposure, although the upper limit is unlikely to be more accurate than a factor of 2. It appears that the most likely explanation of the observed discrepancies is that the line fluxes are near the *IUE* threshold of detectability in the shorter exposures of Simon, Linsky, and Stencel (1982).

TABLE 7

C II EMISSION FROM α TRIANGULI AUSTRALIS

	f_0[a]	
λ	LWR 13980	LWR 13981
2324.6.....	6.3	4.4
2325.4.....	20.2	15.4
2326.9.....	4.3	4.8
2328.1.....	9.2	5.8

[a] Fluxes measured at Earth in units of 10^{-13} ergs cm^{-2} s^{-1}.

Reimer's (1982) line fluxes for ι Aur and θ Her are a factor of 2 larger than ours. It appears that much of the difference is due to the shorter exposure times of Reimers's spectra and different placement of the background levels, which affect the fluxes of weak lines quite considerably. Placement of the continuum level at the long-wavelength ends of the SWP spectra is also complicated by photospheric absorption features. Independent measurements of Reimers's spectra by one of us (A. B.) provide limits to the high-temperature emission which are in better agreement with the values presented in Table 2. Considering the exposure levels involved, there is no real evidence for variability in the high-temperature emission.

III. ATMOSPHERIC STRUCTURE

a) Detection of High-Temperature Gas

There are only small differences in the Mg II/C IV ratio among the four hybrid stars in this sample. This suggests that Mg II flux levels can be used to scale exposures for the purpose of detecting high-temperature emission. C IV emission in α TrA is easily detected in a 1 hr exposure; scaling from the Mg II fluxes, this suggests that the appropriate exposures for γ Aql and ι Aur should be ~3 hr and 4 hr, respectively, if not longer to account for the increasing background. Our results show that 4–6 hr exposures of our program stars are required in order to confirm the C IV emission, and perhaps more importantly, to demonstrate the existence of other high-temperature emission lines.

The results of our long exposures suggest that high-

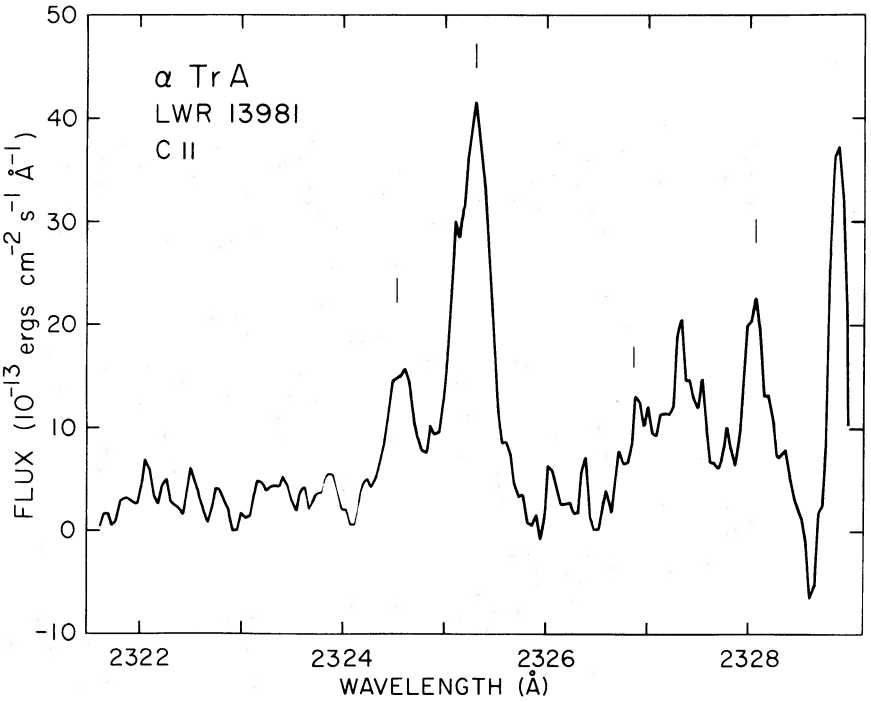

FIG. 8.—The region of the C II] density-sensitive multiplet in α TrA. Lines indicate positions of members of the multiplet.

temperature emission may exist in other stars similar in spectral type to α TrA, but that the sensitivity of *IUE* makes it difficult to observe such emission in all but the brightest objects.

Simon, Linsky, and Stencel (1982) noted four stars in the "cool atmosphere" region of the H-R diagram that also displayed He I λ10830 features. Normally, high temperatures are required to form this line, whether by collisional excitation or photoionization. When they found no high-temperature emission, Simon *et al.* speculated on alternative mechanisms for the formation of λ10830 at low temperatures. We have shown that two of these stars, γ Aql and ι Aur, do in fact exhibit transition region emission, consistent with the observation of He I. A star not considered by Simon, Linsky, and Stencel (1982), θ Her, also exhibits a λ10830 feature (Zirin 1982) as well as C IV emission. We suspect that the other two stars with λ10830 studied by Simon, Linsky, and Stencel (1982), γ Dra and β Oph, also have faint transition-region emission, but the *IUE* exposures were not sufficiently long to detect the lines.

b) *Emission Measure Analysis*

The emission measure distributions were derived from the observed fluxes converted to stellar surface fluxes using angular diameters obtained from colors and the Barnes-Evans relations (Barnes, Evans, and Moffett 1978). A measurement of the angular diameter of ι Aur (7.9×10^{-3} arcsec) made by Blackwell and Shallis (1977) using the infrared flux method is in good agreement with the diameter derived from the Barnes-Evans relation.

The stellar parameters adopted are summarized in Table 8. The absolute magnitudes are those given by Reimers (1982), from Wilson (1976). The stellar radii which result from the angular diameters and absolute and apparent magnitudes are listed, since they are used with the general assumption that $(M/R)_*/(M/R)_\odot = 0.10$ to derive surface gravities. This mass-to-radius ratio is derived from the average properties of K3 II and K4 II stars since a more accurate method is not available.

The stellar surface fluxes of line emission from the four stars differ by small amounts. θ Her has the largest surface fluxes and ι Aur the smallest, but the difference between them is less than a factor of 4. The surface fluxes for γ Aql and α TrA are factors of 3.0 and 1.7, respectively, lower than those of θ Her. The surface averaged fluxes seem to fall about one order of magnitude below the fluxes for the G supergiant hybrid stars α Aqr and β Aqr (Hartmann, Dupree, and Raymond 1980).

The surface fluxes have been used to determine emission measures required to produce the flux in each line as function of T_e. The atomic data are as adopted in earlier work by Brown and Jordan (1981), as updated by Brown, Ferraz, and Jordan (1984) with some further changes. The mean collision strength

TABLE 8

STELLAR PARAMETERS ADOPTED

Star	Spectral Type	m_v	M_v	θ (10^{-3} arcsec)	R/R_0	g (cm s^{-2})
θ Her	K3 II	+2.9	−2.5	3.7	74	36
ι Aur	K3 II	+2.7	−1.5	7.9	59	46
γ Aql	K3 II	+2.7	−1.9	8.0	71	38
α TrA	K4 II	+1.9	−2.4	11.5	89	30

adopted for the Mg II resonance lines is 16.5, the value given by Mendoza (1981) at 10^4 K. The Si II emission measure has been calculated assuming that the ^2D levels are populated only from the ground ^2P levels, since the density is not sufficiently high to give significant excitation from the metastable ^4P levels. The effective cross section for the C II lines at $\sim$1335 Å is further reduced in the recent calculations by Hayes and Nussbaumer (1984) and is now a factor of 2 less than that adopted by Brown and Jordan (1981). The anomalous weakness of the 1335 Å lines noted by Brown, Ferraz, and Jordan (1981) is now therefore understandable.

Initially, solar abundances were adopted, but these lead to a Si III]/C III] ratio which would not be consistent with the densities measured from the C II] lines. Also, the hybrid stars are apparently fairly massive ($M/M_\odot \approx 6$–9; see § IV), evolved stars, and it seems quite possible that dredging up of processed material could alter surface abundances in these objects. We have analyzed the data using two different sets of abundances, as given in Table 9. The "evolved" abundances adopted for C, N, and O are based on several papers (Luck 1978; Luck and Lambert 1981; Lambert and Ries 1981; Bonnell and Bell 1982; Kjaergaad *et al.* 1982) none of which treat the hybrid stars, and the values are simply typical values for evolved stars. Kovacs (1983) gives abundances for Mg, Al, and Si in α TrA, and these are used.

As discussed below, the "evolved" abundances appear to produce more consistent results, although our overall conclusions remain unchanged using solar abundances. Direct abundance measurements for these stars would be quite useful.

The ion balance calculations adopted are for the low-density regime appropriate for these stars (Jordan 1969). Baliunas and Butler (1980) have shown that charge exchange with hydrogen can affect the Si II and Si III ion populations. However, the important influence for Si II is at $T_e \gtrsim 2.5 \times 10^4$ K, whereas the line formation occurs mainly at lower temperatures. Similarly, Si III is affected only at temperatures below 2.5×10^4 K, whereas line formation occurs around 5×10^4 K. Charge exchange with He can increase the Si IV population below 8×10^4 K, and its inclusion would extend the region of line formation to lower temperatures, but the mean emission measure adopted would not be changed (see below). The contribution of this second charge exchange process, as calculated by Baliunas and Butler, will in any case be overestimated owing to the rather large value of $N(\mathrm{He})/N_e$ adopted.

The emission measure used here is

$$E_m(T_e) = 0.88 \int_R N_e^2 dh \,, \qquad (1)$$

where R refers to the region over which about 70% of a line is formed. Assuming $N_\mathrm{H} = 0.8 N_e$, which is valid above $T_e \approx 10^4$ K,

$$E_m(T_e) = 0.7 \int_R N_e N_\mathrm{H} dh \,. \qquad (2)$$

$E_m(T_e)$ then gives the value of E_m at T_e which is required to account for all the line flux. The emission measure analysis follows in a straightforward way for the effectively thin emission lines, following Brown and Jordan (1981).

The loci of emission measures derived for each line are plotted in Figures 9*a* and 9*b*. Figure 9*b* shows the loci for α TrA over a wide temperature range. Fluxes for the lines of C II] at 2325 Å and Al II] at 2670 Å are avilable only for α TrA. The C II] loci are shown for two values of N_e: (a) 10^9 cm^{-3} and (b) 10^8 cm^{-3}. The shape of the distribution between 10^4 K and 10^5 K is constrained by the lines of C II and C IV, irrespective of the carbon abundance. (C III] is in principle density sensitive.) Between 6300 K and 1.5×10^4 K a self-consistent mean curve can reproduce Mg II and C II]. The Mg II locus may be too low, since no allowance has been made for interstellar absorption. The Si II locus appears to be too high by a factor of up to 3. A more sophisticated calculation of the collision strength for the ^2P–^2D Si II transition is urgently required. The Al II] locus lies below that of Mg II, but both the fluxes and atomic data are less certain.

The Si IV and N V fluxes are difficult to measure accurately. The Si IV lines are weak, and the apparent N V lines may contain contributions from C I lines near the series limit and from the wing of the strong geocoronal Lyα emission. Hartmann, Dupree, and Raymond (1981) drew attention to the relatively large surface fluxes of N V lines in the hybrid stars compared with the Sun. Although, as they suggest, this might indicate a real difference in the shape of the emission measure distribution, a higher N abundance might also be the cause. Above 1.6×10^4 K the mean curves gives a good fit to all the lines, only Si IV lying 0.2 dex high. However, if solar abundances are adopted, the scatter is increased. The Si II, Si III], and Si IV curves and N V would all be raised, while those of C II, C III], and C IV would be lowered. However, the differences in the final models are within the uncertainties associated with the surface fluxes and atomic data.

Figure 9*b* shows the results for ι Aur, γ Aql, and θ Her on offset scales for clarity, and restricted loci. However, the close similarity of the shape of all of the emission measure distributions is apparent.

If the nitrogen abundance is high, then the flux in the N III] 1750 Å multiplet is predicted to be about 0.2–0.4 times that of the C III] 1909 Å line. Our spectra, and the low-dispersion spectrum of α TrA (Hartmann, Dupree, and Raymond 1982) show a feature at 1750 Å which suggests emission with an even larger flux. Since several other lines may contribute to this emission (e.g., Fe II, Ni II), and it is difficult to set the continuum level, the evidence for enhanced N III] is inconclusive. Deeper high-resolution spectra are required to settle the matter.

The absence of any correction for interstellar absorption will lead to the mean distributions being underestimates. Because of the wavelength dependence of the mean extinction curve, the *shape* of the emission-measure distribution is not strongly dependent on the extinction. It is difficult to determine extinction corrections for these stars. Comparison of the observed colors with the mean relations as a function of spectral type presented by Johnson (1966) suggest $E_{B-V} \approx 0.1$, correspond-

TABLE 9

ABUNDANCES ADOPTED

Element	N_E/N_H (solar)	N_E/N_H (evolved)
C	2.5×10^{-4}	1.4×10^{-4} [a]
N	8.0×10^{-5}	2.1×10^{-4} [a]
O	6.3×10^{-4}	6.3×10^{-4} [a]
Mg	4.0×10^{-5}	5.8×10^{-5} [b]
Al	2.5×10^{-6}	2.1×10^{-6} [b]
Si	4.0×10^{-5}	5.4×10^{-5} [b]

[a] Typical values (see references in text).
[b] From Kovacs 1983.

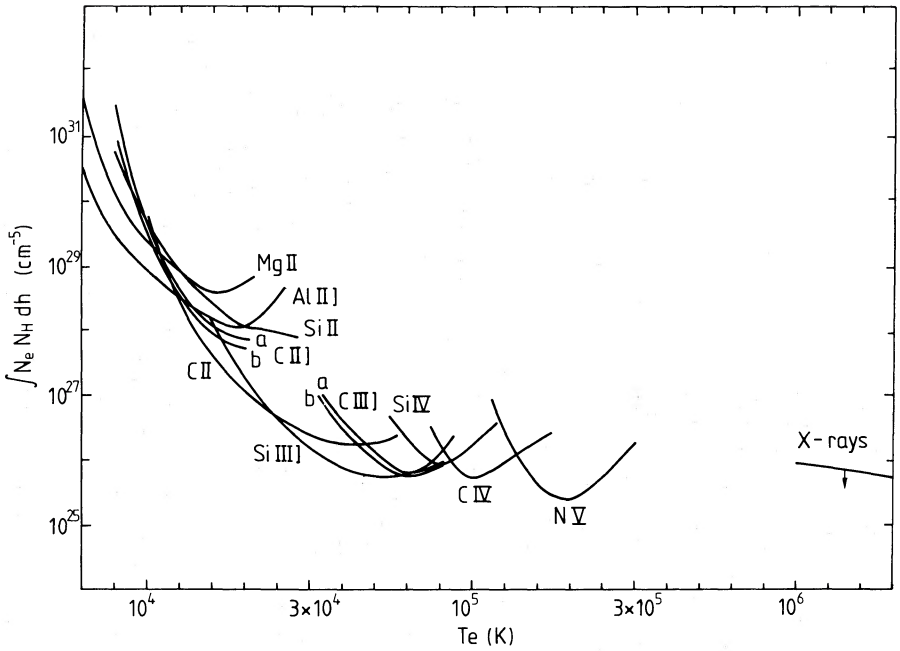

FIG. 9*a*.

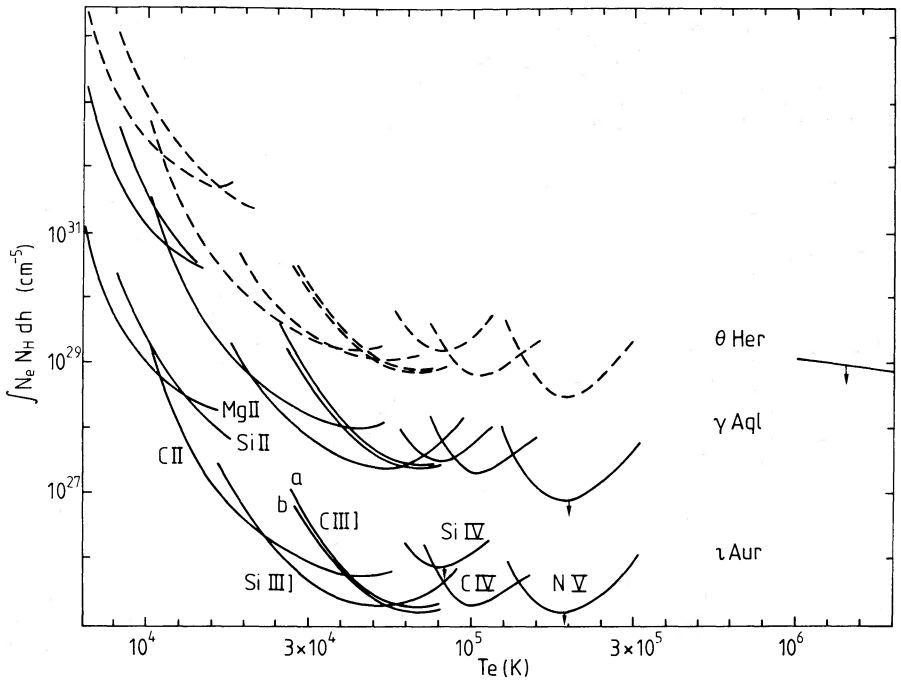

FIG. 9*b*.

FIG. 9.—(*a*) Emission measure loci, $\int N_e N_H dh$ vs. T_e, for α TrA. The curves (a) and (b) for C II] and C III] refer to $N_e = 10^9$ cm^{-3} and 10^8 cm^{-3}, respectively. The upper limit above 10^6 K is scaled from θ Her. (*b*) Emission measure loci for ι Aur, θ Her, and γ Aql. The vertical scale is for ι Aur; the curves for γ Aql and θ Her are increased by two and three orders of magnitude, respectively, for clarity.

ing to a factor of 2 correction in the short-wavelength region. The fact that all of the K-type hybrid stars have uncorrected surface fluxes within a factor of 4 of each other makes it unlikely that much larger extinction corrections must be applied to the observed fluxes.

The mean emission measures are given in Table 10 on the absolute scale for α TrA. The factors by which the distributions for the other stars should be scaled are 1.7 (θ Her), 0.6 (γ Aql), and 0.4 (ι Aur).

The locus above 10^6 K shown in Figure 9*a* is consistent with the observed 1640 Å fluxes. In α TrA, about 3% of the total low-resolution flux at this wavelength is due to He II emission. Assuming that 90% of this emission is formed by recombination, Hartmann, Dupree, and Raymond (1981) deduced an upper limit to the "coronal" emission measure of $\sim 10^{26}$ cm^{-5}. This upper limit is still appropriate. *HEAO 2* measurements can be used to provide upper limits to the amounts of gas at temperatures $T \gtrsim 3 \times 10^6$ K. The emission measure

TABLE 10

MEAN EMISSION-MEASURE DISTRIBUTION FOR α TRIANGULI AUSTRALIS

log T	log $\int N_e N_H dh$	log T	log $\int N_e N_H dh$
3.8.....	31.60	4.7.....	25.77
3.9.....	30.00	4.8.....	25.75
4.0.....	29.15	4.9.....	25.75
4.1.....	28.40	5.0.....	25.75
4.2.....	27.62	5.1.....	25.65
4.3.....	27.00	5.2.....	25.50
4.4.....	26.45	5.3.....	25.30
4.5.....	26.10	6.0.....	25.95
4.6.....	25.83		

distribution of Figure 9*a* is consistent with the upper limit to the X-ray flux from γ Aql, $f_x < 2 \times 10^{-13}$ ergs cm^{-2} s^{-1}, reported by Haisch and Simon (1982). The upper limit for α TrA has been scaled according to the C IV fluxes. There is a marginal detection of θ Her by Caillault and Helfand (1983) of $f_x \approx 2.1 \times 10^{-13}$ ergs cm^{-2} s^{-1}, which leads to the same scaling factor of 1.7 between the X-ray fluxes of α TrA and θ Her. Preliminary modeling of the Mg II and Ca II line profiles of hybrid stars by Hartmann, Avrett, and Dupree (1985) suggests that the mass-loss rates are sufficiently low that circumstellar absorption of X-rays is unlikely to be significant for energies $\gtrsim 1$ keV (cf. also Drake and Linsky 1984).

Although the flux in the Bα line of He II at 1640 Å provides an upper limit to coronal photoionizing fluxes, the observed emission may be produced by collisional excitation at $T_e \approx 8 \times 10^4$ K. In the optically thin limit, the emission measure at this temperature fails to account for the Baα flux by a factor of 13. If the optical depth in Lyβ is sufficiently large, conversion to Baα can increase the expected emission by up to a factor of ~4. This seems to be inadequate to explain the observed flux in α TrA, although the absence of high-resolution observations for the other hybrid stars does not permit separation of the 1640 emission into He II and O I components.

c) *Electron Densities*

The electron density can be investigated through the ratios of lines within the C II] multiplet at 2325 Å using the calculations published by Stencel *et al.* (1981). This method has the advantage that it does not depend upon the carbon abundance, nor are the results strongly dependent on T_e in the range 7000 K–(2×10^4) K. Adopting $T_e = 1.3 \times 10^4$ K (from Fig. 8*a*), the best measured line ratio, ($^2P_{3/2}$–$^4P_{5/2}$/$^2P_{1/2}$–$^4P_{1/2}$) leads to $N_e = (2.9 \pm 2) \times 10^8$ cm^{-3}.

If $N_e T \leq 3.6 \times 10^{12}$ cm^{-3} K at 6.3×10^4 K, the optimum temperature for the formation of C III] 1909 Å, then the C III $^3P_1$ level should decay predominantly by spontaneous radiation and the Si III]/C III], 1892 Å/1909 Å flux ratio should not be dependent upon N_e, but should have its low density limit value. Adopting the most recent collision strengths (Dufton *et al.* 1978; Baluja, Burke, and Kingston 1980, 1981), low-density ion balance populations at $T_e = 5 \times 10^4$ K and 6.3×10^4 K for C III and the solar abundances given in Table 9, we find a line ratio of 0.44. The emission measure is assumed to be the same for both ions, on the basis of the mean curves shown in the figures. A higher value (~0.8) could be obtained if both lines were formed at $T_e \approx 5 \times 10^4$ K.

The ratio for α TrA, which can be measured accurately from high-dispersion spectra, is ~1. The approximate ratios from the low-dispersion spectra of ι Aur and γ Aql are ~1.3, and that from θ Her is ~2. However, it should be noted that the measured fluxes are extremely uncertain, due to blends with the nearby S I lines and especially because of the difficulty of removing the substantial photospheric background (Fig. 1). Thus, although the results are only marginally significant, the observed ratios are higher than the best estimate of the low-density limit. If some dredging up of processed material has occurred, then the true low-density ratio of Si III]/C III] will be larger. A relative underabundance of C to Si of a factor of 2 could therefore account for the apparent difference in P_e between the C II] and the Si III]/C III] ratios.

A further constraint is placed on N_e by the observed upper limit to the flux in the C III quadrupole line, ($2s^2\ ^1S_0$–$2s2p\ ^3P_2$) at 1906.7 Å. The ratio of this line to the intersystem line is ≤0.1, showing that $N_e \geq 10^6$ cm^{-3} at 5×10^4 K (Nussbaumer and Schild 1979; Keenan *et al.* 1984).

An alternative, though crude, method of investigating N_e is to use the ratio of opacity-sensitive lines to determine $\int N_H dh$ and then combine this with the emission measure in the form $\int N_e N_H dh$ (Jordan and Brown 1981). Two sets of lines can be used in α TrA. The ratio of the flux in the O I intercombination line at 1641.3 Å to that in the O I line at 1304.87 Å, which is unaffected by interstellar absorption, yields the opacity in the line at 1304.87 Å. Similarly, the ratio of the flux in the C I intercombination line at 1993.6 Å to that in the multiplet at 1656 Å yields the opacity in the latter multiplet.

The intersystem line fluxes (Table 3) are from the high-resolution spectra. The permitted line fluxes are one-third and one-sixth of the total low-resolution fluxes for the O I and C I multiplets, respectively. These will be lower limits, since interstellar absorption is expected for the multiplet components originating from the zero volt energy level.

Calculating the line center opacity for Doppler-broadened lines, assuming Boltzmann distribution populations for the ground-term levels, and on the basis of ion balance calculations, we find similar upper limits to the column densities of O I and C I. Taking thermal broadening at $T_e \gtrsim 6000$ K as a lower limit to the line width leads to a mean column density in the range $5 \times 10^{20} < \int N_H dh < 3 \times 10^{21}$ cm^{-2} (cf. Table 11). The column density can be combined with the emission measure, $\int_{\Delta H} N_e N_H$, in the temperature range 6300–10^4 K to place approximate limits on N_e. These are given in Table 11.

TABLE 11

PARAMETERS DETERMINED FROM OPACITY-SENSITIVE RATIOS AND EMISSION MEASURES

log T (K)	$\int N_H dh$ (cm^{-2})	N_e (cm^{-3})	ΔH (cm)	N_H (cm^{-3})
3.8.....	(5.2–30) × 10^{20}	(7.7–1.3) × 10^{10}	2.7 × 10^{10}	(1.9–1.1) × 10^{10}
3.9.....	(5.9–30) × 10^{20}	(1.7–0.33) × 10^9	3.1 × 10^{10}	(1.9–9.9) × 10^{10}
4.0.....	(6.6–30) × 10^{20}	(2.1–0.47) × 10^8	3.5 × 10^{10}	(1.9–8.7) × 10^{10}

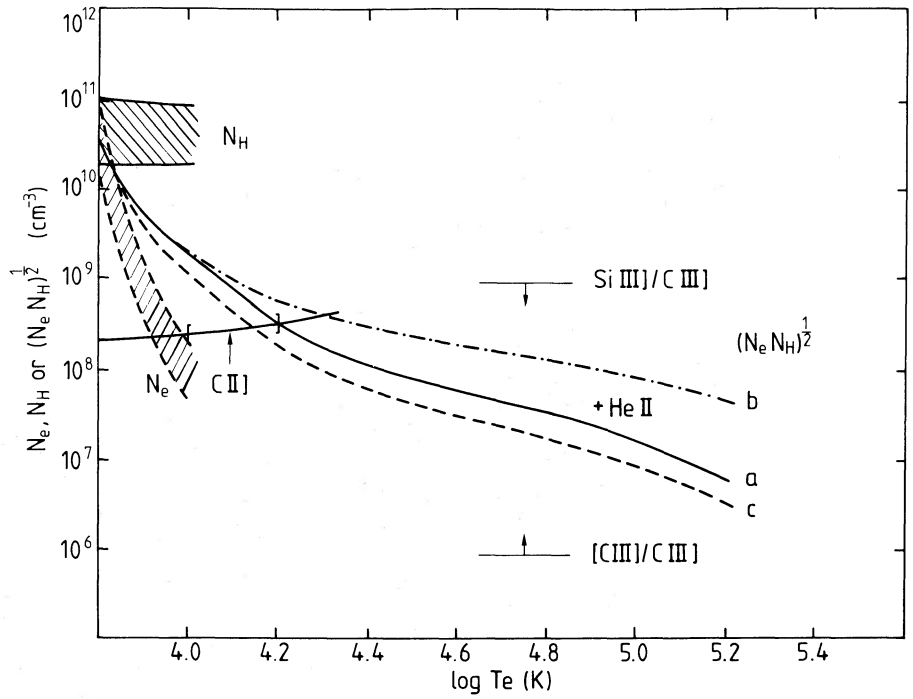

FIG. 10.—Summary of variation of N_e with T_e and observational constraints for α TrA. The lines labeled a, b, and c refer to the cool static, hot static, and turbulently extended models listed in Table 12 and give $(N_e N_H)$. Upper and lower limits on N_e at $T_e \approx 5.6 \times 10^4$ K are provided by the Si III and C III intersystem lines and the C III magnetic quadrupole line. Opacity sensitive ratios of C I and O I limit N_H and N_e at low temperatures. The range indicated by shading arises through uncertainty in T_{ion}. The C II] lines give a locus for N_e, the emission measure distribution giving an "optimum" range of formation indicated by the brackets.

The results of the various methods of estimating N_e are summarized in Figure 10.

d) Minimum Pressure Hydrostatic Models

The pressure as a function of temperature cannot be found without making further assumptions. First, we adopt hydrostatic equilibrium. Since the temperature gradient can be expressed as

$$dT_e/dh = P_e^2/[2E_m(T_e)T_e] , \quad (3)$$

this can be combined with dP_e/dh in hydrostatic equilibrium to yield

$$P_e^2 = P_T^2 + 2.8 \times 10^{-8} g_* \int_{T_e}^{T_T} E_m(T_e) dT_e . \quad (4)$$

P_T is the pressure at the highest observed temperature. The minimum pressure model can be found by taking $P_T = 0$ at some temperature, taken here as 2×10^5 K. Higher pressure models can easily be made by using a higher starting pressure. If turbulence or flows are taken into account, lower pressures will result. The minimum (static) pressure model for α TrA is given in Table 12. Since the minimum pressure scales as $[g_* E_m(T_e)]^{0.5}$ and these stars have the same relative emission measure distribution, the pressure at each temperature will scale between the stars by constant factors. For the other hybrid stars, the factors are 1.4 (θ Her), 0.83 (ι Aur), and 0.83 (γ Aql).

Figure 11 shows the minimum pressure, hydrostatic models for α TrA starting at log $T = 5.3$ and log $T = 6.0$. For the latter model a simple linear interpolation of the emission measure between log $T = 5.3$ and 6.0 has been used.

e) Turbulent Support and Atmospheric Extension

The observed widths of optically thin lines of C II, Si III, and C III show that the mass motions correspond to velocities about 1.6 times the thermal velocities (of hydrogen). Thus the turbulent motions will give an additional support term that is equivalent to reducing the effective gravity. Equation (4) relates the pressure variation to the emission measure and gravity. If

TABLE 12

PRESSURES IN EXAMPLE MODELS FOR TRIANGULI AUSTRALIS

	P_e (cm^{-3} K)		
LOG T (K)	(a) Static Model	(b) Static Model Extending to 10^6 K	(c) Model with "Turbulent" Support
3.8[a]	2.7(14)	2.7(14)	2.7(14)
3.9[a]	5.1(13)	5.2(14)	3.4(13)
4.0	2.3(13)	2.4(13)	1.3(13)
4.1	1.1(13)	1.4(13)	6.0(12)
4.2	5.9(12)	1.1(13)	3.2(12)
4.3	4.1(12)	1.0(13)	2.2(12)
4.4	3.4(12)	9.0(12)	1.8(12)
4.5	3.0(12)	8.9(12)	1.6(12)
4.6	2.9(12)	8.8(12)	1.4(12)
4.7	2.7(12)	8.8(12)	1.2(12)
4.8	2.6(12)	8.7(12)	1.2(12)
4.9	2.4(12)	8.7(12)	1.1(12)
5.0	2.1(12)	8.6(12)	9.8(11)
5.1	1.7(12)	8.5(12)	8.2(11)
5.2	1.2(12)	8.4(12)	8.2(11)
6.0	...	5.0(12)	...

[a] Approximate values assuming $N_H = 0.8 N_e$.

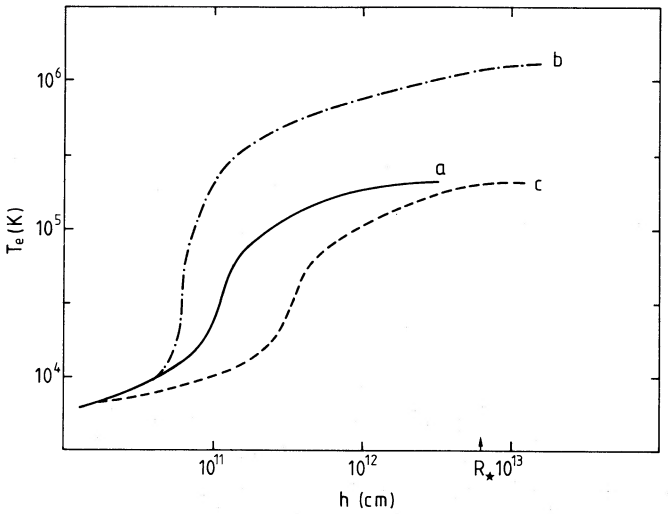

FIG. 11.—The temperature structure of the three models of α TrA: (a) static, cool, model; (b) static, hot model; and (c) turbulently supported cool model.

we assume for simplicity that the turbulent pressure is a fixed factor of 2.5 times the gas pressure, then the effect of the turbulent support appears only in the replacement of g_* by $g_{\rm eff} = g_*/3.5$. In the minimum pressure model, the pressure above $\log T = 5.3$ is taken as zero and thus the values of P_e^2 found at lower temperatures are reduced by a factor of 3.5. [In practice the observed variation of $P(\text{total})/P_g$ can be and was included in the integration over temperature.] Figure 11 shows both the minimum pressure hydrostatic model and the turbulently supported hydrostatic model (cf. Table 12). The reduction of N_e by a factor or less than 2 makes no significant difference to the conclusions derived from density-sensitive line ratios. The C II] lines still produce a solution at a reasonable temperature. The model will be only approximate above $\sim 10^5$ K because the analysis cannot take into account the unknown radial extent of this region; we assume $r \approx R_*$.

In the static model, the thickness of the region around 1.6×10^5 K is 0.16 R_*; the inclusion of turbulence increases this to at least 0.6 R_*. Thus the layer that in the Sun is a narrow "transition region" is probably more appropriately described as a "warm corona" in the hybrid stars.

We conclude that the observed emission-measure distribution, interpreted in terms of a turbulently extended atmosphere near hydrostatic equilibrium, produces a simple one-component model consistent with the constraints provided by the opacity and density-sensitive line ratios. Of course, higher pressure and temperature models would result if the emission were restricted to only a fraction of the stellar atmosphere.

f) Line Opacities

The models can be used to estimate the opacity effects in the observed lines. The C III] and Si III] lines are optically thin, and their great width must be due to a supersonic velocity field. It is found that the lines of C II and C IV have minimum line center optical depths $\tau \approx 8$ and 1, respectively. (Note that a substantial circumstellar shell optical depth in C II is not ruled out). Since there is no destruction of photons, only scattering, the effects of these opacities will be to broaden the emission lines. The O I and Mg II lines are clearly very optically thick; the estimated values are $\tau_0 \approx 10^3$ and 10^4, respectively.

IV. ENERGY BALANCE, WAVE FLUXES, AND WINDS

a) Mechanical Energy Fluxes

The radiative losses, which can be derived from the emission-measure distribution as a function of temperature, provide constraints on the amount and pattern of mechanical energy deposition. Because the scale heights of the model atmospheres are so large, thermal conduction is negligible. (The only way around this result is to assume that we have underestimated the relevant densities by more than two orders of magnitude, which seems unlikely.) Thus the energy balance is maintained between local radiation losses, energy lost in expansion, and local nonthermal heating. The radiation losses can be found by summing

$$\Delta F_R = 0.37 E_m(T_e) P_{\rm rad} , \qquad (5)$$

where $P_{\rm rad}$ is the radiative loss per $N_e N_{\rm H}$ at T_e. The resulting distribution is shown in Figure 12 as the cumulative sum of radiative losses proceeding from high to low temperatures.

The distribution of $\sum \Delta F_R$ with T_e can be compared with possible wave energy fluxes for different modes, computed by multiplying the nonthermal energy density $0.5\rho v_{\rm turb}^2$ by (*i*) the sound speed, (*ii*) the turbulent velocity, or (*iii*) the Alfvén speed. Propagation at either the turbulent velocity or the sound speed provides insufficient energy flux. The energy requirements can be satisfied by the Alfvén speed if field strengths of a few gauss are adopted. This is also comparable to the field strengths required to drive acceptable mass-loss rates (cf. Hartmann, Dupree, and Raymond 1981).

b) Wave-driven Wind Models

The large widths of the Si III] and C III] lines indicate that turbulent pressure is more important than thermal pressure in the transition region. Hartmann, Dupree, and Raymond (1981) suggested that Alfvén waves might produce warm winds from hybrid stars, and that the observed transition-region lines are broadened by outflow. As noted above, the mechanical energy fluxes required to heat the atmosphere are comparable to those required to drive substantial mass loss.

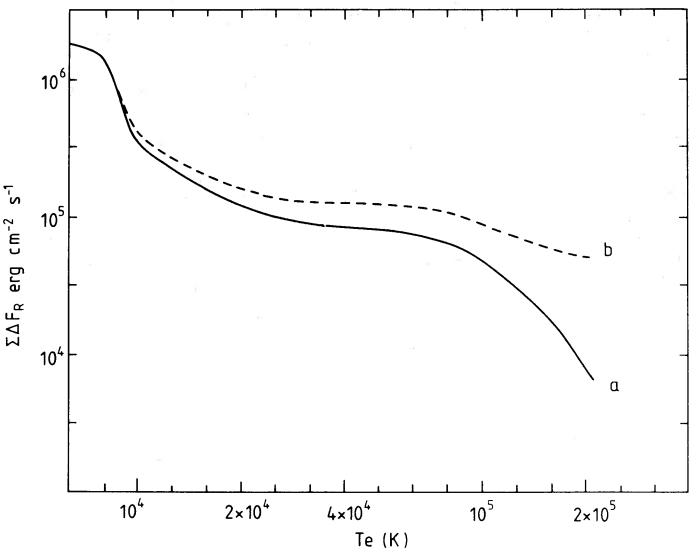

FIG. 12.—The variation of $\sum \Delta F_R$ (ergs cm^{-2} s^{-1}) with temperature. The curves (a) and (b) refer to models starting at 2×10^5 K and 10^6 K, respectively.

The absence of line shifts, coupled with the radial extent of the transition region estimated from the models of the previous sections, suggesting that turbulent broadening dominates the expansion velocity in the region(s) where Si III and C III are formed. Although the observations are consistent with static models including turbulent pressure, the absence of significant shifts in the line profiles is also consistent with the Alfvén wave-driven wind model constructed by Hartmann, Dupree, and Raymond (1981). The reason is that in the inner regions of the flow, wave amplitudes are much larger than the expansion velocity (see also Hartmann, Edwards, and Avrett 1982), and so the line broadening is produced principally by wave motion.

The simple wind model presented by Hartmann, Dupree, and Raymond (1981; Model B) cannot account for the observed N V emission, since the maximum temperature is less than 10^5 K. In addition, the densities indicated by the C II] lines are substantially higher than in the wind model. Recent calculations for more appropriate stellar parameters (Mendoza-Ortega and Jordan 1985) suggest that below 10^5 K there may be no conflict between a model which extends to a high-velocity wind and that described by the inclusion of a turbulent support term, since in this temperature range flow effects are not important in the energy balance, i.e., the atmosphere may be considered as a mildly expanding, turbulently supported atmosphere out to $\sim 1\ R_*$, extending into a high-velocity wind at greater distances.

Analogy with the Sun suggests that the bulk of the emission may arise from magnetically closed regions. However, even if the UV emission is not directly connected with outflow, the large "turbulent" broadening observed suggests that "wave" motions are present in the outer envelope at a dynamically important level and may play a role in driving mass loss.

c) *High-Velocity Winds*

The Mg II absorption shift of about -180 km s^{-1} in α TrA represents one of the largest expansion velocities observed in hybrid stars. Reimer's (1982) observations of 12 Peg (K0 Ib) indicated Ca II K absorption with outflow velocities of at least 150 km s^{-1} relative to the photosphere. O'Brien (1980) reported He I 10830 Å absorption in α Aqr at one epoch which reached velocities of -200 km s^{-1}. However, it seems likely that λ10830 is formed relatively close to the star, since high-temperature material is required to populate the lower atomic level by either recombination or collisional excitation, while the Mg II absorption is more likely to reflect the wind at large distances.

The disappearance of emission on the short-wavelength side of the Mg II lines in θ Her and γ Aql suggest that winds with velocities $\gtrsim 120$ km s^{-1} are fairly common from hybrid stars. It is clear that selection effects tend to bias observed wind velocities to lower values, since detection of the high-velocity absorption in the weak Mg II line wings is difficult. (Although the wings of the Ca II resonance lines are much brighter than the Mg II line wings, the circumstellar shell optical depths in the Ca II lines are generally substantially less than in Mg II.)

These results are especially interesting, since theories of mass loss generally have difficulty in producing winds with terminal velocities much less than the escape velocity (cf. Holzer, Leer, and Flå 1983). Our observations indicate that winds with velocities close to the surface escape velocities ~ 200 km s^{-1} characteristic of hybrid stars are observed.

V. EVOLUTIONARY STATUS OF HYBRID STARS

The evolutionary state of cool giant stars has been discussed recently by Simon (1984). He concluded that stars making their first crossing of the Hertzsprung gap have relatively strong transition region emission. Simon, Linsky, and Stencel (1982) suggested that the hybrid stars like α TrA might be first crossing objects as well, although Baird *et al.* (1975) suggested that one known hybrid, β Aqr, is older.

The mass estimates for the hybrid stars fall in the range 4–10 $M_\odot$. Evolutionary tracks (Iben 1966*a*, *b*) show that the K3–4 II hybrids could be near the end of their left-to-right crossing of the H-R diagram, in the region where the outer convection zone deepens as the star begins the ascent of the giant branch. In this location, a lower than solar C/N abundance could be appropriate.

The calculations of Endal and Sofia (1979) suggest that if the K hybrids are first crossing stars, they may be rotating at velocities of ~ 6 km s^{-1} or more. Thus it is possible that part of the wind variability observed on time scales of a year may be due to rotational modulation, if the wind is not accelerated uniformly over the surface. Careful photospheric line broadening measurements could be employed to test this suggestion. Spectroscopy or photometry of the Ca II H and K lines might also reveal periodic modulation by rotation.

Throughout this paper we have assumed that α TrA is a bright giant (luminosity class II) on the basis of the large Mg II line width, using the Wilson-Bappu effect (Hartmann, Dupree, and Raymond 1981). Kovacs (1983) and Holweger and Kovacs (1984) consider α TrA as a K4 III star. Since the gravity found from the Fe I and Fe II lines is essentially the same as adopted here, the difference in interpretation does not affect the atmospheric modeling, only the interpretation of the evolutionary state. The low carbon abundance is consistent with either a K4 II or III star beyond the first dredge-up phase, the moderately high barium abundance found by Holweger and Kovacs (1984) may indicate a later stage of evolution.

It has been recognized that many barium stars are binaries with white dwarf companions (McClure, Fletcher, and Nemec 1980), such as 56 Peg (K0 Ib; Schindler *et al.* 1982) and ζ Cap (G8III; Böhm-Vitense 1980). In this case the evolutionary status is less clear, since as McClure, Fletcher, and Nemec (1979) discuss, the barium anomaly may arise through mass exchange rather than mixing. The evolutionary development of intermediate-mass binaries has been recently discussed by Iben and Tutukov (1984).

In the case of 56 Peg, it has been suggested that the transition-region emission from this wide binary arises from the influence of the white dwarf, probably by photoionization of the wind (Schindler *et al.* 1982). We see no evidence for a hot white dwarf in any of the hybrid SWP spectra. The number of bright hybrid stars that have been found, coupled with the difficulty of detection, suggests that such stars are fairly common, and makes it unlikely that the ionizing effects of hot white dwarfs account for the hybrid phenomenon.

Ayres (1985) has recently suggested that α TrA may be a binary, based on a claim of ultraviolet continuum excess. Ayres has also proposed that the transition-region emission arises from the suggested F dwarf companion. It is difficult to assess the continuum properties of cool, heavily blanketed stellar photospheres at such short wavelengths. The required surface fluxes are extremely high, at levels not observed from any other such main-sequence star. Finally, the low atmospheric pres-

sures derived here are not consistent with the high pressures associated with very active stars. Even if such an object is invoked to explain α TrA's activity, it seems unlikely that all of the other known hybrid stars—α Aqr, β Aqr, ι Aur, γ Aql, and θ Her—can be explained by this model.

There has been some discussion in the literature as to how the hybrids fit into the picture of a sharp "dividing line" separating stars which do or do not show C IV emission (Linsky and Haisch 1979; Simon, Linsky, and Stencel 1982; Haisch and Simon 1982; Hartmann, Dupree, and Raymond 1980, 1981; Reimers 1982). Since there is no reason why a straight line should connect the regions of the H-R diagram at which sufficient nonthermal energy exists to produce transition-region temperatures, the argument has become sterile. It is clear that at some point the C IV flux becomes too weak to observe in the supergiants and giants. These two regions can be joined by a straight line, but there is no *a priori* reason that it should cross the point where the decrease in transition-region emission occurs for intermediate mass stars. Indeed, the hybrids suggest that this is not the case.

Middelkoop (1982) has reported Ca II chromospheric indices for a large survey of evolved, late-type stars. He found that giants with masses $\sim 2\ M_\odot$ or less exhibited a sharp decrease in chromospheric emission at $B-V \approx 0.95$, close to the position of the dividing line (Simon, Linsky, and Stencel 1982). Simon (1984) has shown similar behavior in C IV. However, Middelkoop found no well-defined break in emission from stars with $M \approx 3$–$5\ M_\odot$. These data suggest a substantial decline in magnetic activity occurs near the dividing line for low-mass stars, but not for high-mass stars. This is consistent with our interpretation of hybrid objects as massive stars, explaining their anomalous position in the H-R diagram relative to the low-mass giants.

VI. CONCLUSIONS

We have confirmed the high-temperature emission in two suspected hybrid atmosphere stars and have discovered a new hybrid object. These results indicate that hybrid stars may be relatively common, but that the discovery of further members of the class requires very long exposures with *IUE*.

The emission line fluxes have been used to construct an emission measure distribution. Various line ratios have been used to constrain the range of acceptable electron pressures. The analysis indicates that at $\sim 10^5$ K, the pressure is between 10^{-2} and 10^{-3} that in the solar atmosphere at the same temperature. A corona with average temperature up to $\sim 5 \times 10^5$ K could be accommodated. The observed line widths indicate that turbulent pressure is important. The emission lines are not inconsistent with a small expansion of the atmosphere in the line formation region. Low carbon abundances typical of evolved giants improve the consistency of the emission measure distribution and Si III]/C III] line ratios. Acoustic wave heating is not sufficient to balance the observed radiative losses.

Very high-speed Mg II circumstellar absorption was discovered in the hybrid star α TrA. These spectra, along with observations of the other hybrids, suggest that variable wind velocities of 100–200 km s^{-1} may be common, but previous searches have strong selection effects against observing high-velocity absorption.

The hybrid stars appear to be at least in the first dredge-up stage of giant evolution and may be at more advanced stages, depending upon the interpretation of the overabundance of barium in α TrA.

We gratefully acknowledge the support of the *IUE* observatory staff at both NASA/Goddard and at the ESA ground station at Villafranca in obtaining the data reported here. We also acknowledge useful comments from John Raymond, particularly concerning the N III] and He II emission lines. This work was supported by NASA grant HAG 5–87 to the Smithsonian Astrophysical Observatory, by NASA grant NAG 5-82 to the University of Colorado, and by the U.K. SERC.

REFERENCES

Ake, T. B. 1981, *IUE NASA Newsletter*, No. 15, p. 60.
Ayres, T. R. 1985, *Ap. J. (Letters)*, **291**, L7.
Ayres, T. R., Linsky, J. L., Simon, T., Jordan, C., and Brown, A. 1983, *Ap. J.*, **274**, 801.
Ayres, T. R., Moos, H. W., and Linsky, J. L. 1981, *Ap. J. (Letters)*, **248**, L137.
Baird, S. R., Roberts, W. J., Snow, T. P., and Wallerstein, G., 1975, *Pub. A.S.P.*, **87**, 385.
Baliunas, S. L., and Butler, S. E. 1980, *Ap. J. (Letters)*, **235**, L45.
Baluja, K. L., Burke, P. G., and Kingston, A. E., 1980, *J. Phys. B.*, **13**, L543.
———. 1981, *J. Phys. B.*, **14**, 1333.
Barnes, T. G., Evans, D. S., and Moffett, T. J. 1978, *M.N.R.A.S.*, **183**, 285.
Blackwell, D. E., and Shallis, M. J. 1977, *M.N.R.A.S.*, **180**, 177.
Boggess, A., *et al.* 1978, *Nature*, **275**, 361.
Bohlin, R., and Holm, A. 1980, *IUE NASA Newsletter*, No. 10, p. 37.
Böhm-Vitense, E. 1980, *Ap. J. (Letters)*, **239**, L79.
Bonnell, J., and Bell, R. A. 1982, *M.N.R.A.S.*, **201**, 253.
Brown, A., and Jordan, C. 1981, *M.N.R.A.S.*, **196**, 757.
Brown, A., Ferraz, M. C. de M. and Jordan, C. 1981, in *The Universe at Ultraviolet Wavelengths, The First Two Years of IUE*, ed. R. D. Chapman and A. Boggess (NASA-CP 2167), p. 297.
Brown, A., Jordan, C., and Wilson, R. 1979, in *The First Year of IUE*, ed. A. J. Willis (London: University College London), p. 232.
Caillault, J. P., and Helfand, D. 1983, as quoted in Linsky, J. L. 1983, *Adv. Space Res.*, **2**, 249.
Carpenter, K. G., and Wing, R. F. 1979, *Bull. AAS*, **11**, 419.
Cassatella, A., Ponz, D., and Selvelli, P. L. 1981, *ESA IUE Newsletter*, No. 10, p. 31; and *NASA IUE Newsletter*, No. 14, p. 170.
Drake, S. A., Brown, A., and Linsky, J. L. 1984, *Ap. J.*, **284**, 774.
Drake, S. A., and Linsky, J. L. 1984, in *Third Cambridge Workshop on Cool Stars, Stellar Systems, and the Sun*, ed. S. L. Baliunas and L. Hartmann (Heidelberg: Springer), p. 350.
Dufton, P. L., Berrington, K. A., Burke, P. G., and Kingston, A. E. 1978, *Astr. Ap. Phys.*, **62**, 111.
Endal, A. S., and Sofia, S. 1979, *Ap. J.*, **232**, 531.
Haisch, B. M., and Simon, T. 1982, *Ap. J.*, **263**, 252.
Hartmann, L., Avrett, E., and Dupree, A. K. 1985, in preparation.
Hartmann, L., Dupree, A. K., and Raymond, J. C. 1980, *Ap. J. (Letters)*, **236**, L143.
———. 1981, *Ap. J.*, **246**, 193.
———. 1982, *Ap. J.*, **252**, 214.
Hartmann, L., Edwards, S., and Avrett, E. 1982, *Ap. J.*, **261**, 279.
Hartmann, L., and MacGregor, K. B. 1980, *Ap. J.*, **260**, 242.
Harvel, C. A., Turnrose, B. E., and Bohlin, R. C. 1979, *IUE NASA Newsletter*, No. 5.
Hayes, M. A., and Nussbaumer, H. 1984, *Astr. Ap.*, **134**, 193.
Holweger, H., and Kovacs, N. 1984, *Astr. Ap.*, **132**, L5.
Holzer, T., Leer, E., and Flå, T. 1983, *Ap. J.*, **275**, 808.
Iben, I. Jr. 1966*a*, *Ap. J.*, **143**, 483.
———. 1966*b*, *Ap. J.*, **143**, 505.
Iben, I. Jr., and Tutukov, A. V. 1984, in *Stellar Nucleosynthesis*, ed. C. Chiosi and A. Renzini (Dordrecht: Reidel), p. 181.
Johansson, S., and Jordan, C. 1984, *M.N.R.A.S.*, in press.
Johnson, H. L. 1966, *Ann. Rev. Astr. Ap.*, **4**, 193.
Jordan, C. 1969, *M.N.R.A.S.*, **192**, 501.
Jordan, C., and Brown, A. 1981, in *Solar Phenomena in Stars and Stellar Systems*, ed. R. M. Bonnet and A. K. Dupree (Dordrecht: Reidel), p. 199.
Keenan, F. P., Berrington, K. A., Burke, P. G., Kingston, A. E., and Dufton, P. L. 1984, *M.N.R.A.S.*, **207**, 459.
Kjaergaard, P., Gustafsson, B., Walker, G. A. H., and Hultquist, L. 1982, *Astr. Ap.*, **115**, 145.
Kovacs, N. 1983, *Astr. Ap.*, **120**, 2.
Lambert, D. L., and Ries, L. M. 1981, *Ap. J.*, **248**, 228.

Linsky, J. L., and Haisch, B. M. 1979, *Ap. J. (Letters)*, **229**, L27.
Luck, E. 1978, *Ap. J.*, **219**, 148.
Luck, E., and Lambert, D. L. 1981, *Ap. J.*, **245**, 1018.
McClure, R. D., Fletcher, J. M., and Nemec, J. M. 1980, *Ap. J. (Letters)*, **238**, L35.
Mendoza, C. 1981, *J. Phys. B.*, **14**, 2465.
Mendoza-Ortega, C., and Jordan, C. 1985, in preparation.
Middelkoop, F. 1982, *Astr. Ap.*, **113**, 1.
Nussbaumer, H., and Schild, H. 1979, *Astr. Ap.*, **75**, L17.
O'Brien, G. 1980, Ph.D. Thesis, University of Texas at Austin.
Reimers, D. 1977, *Astr. Ap.*, **57**, 395.
———. 1982, *Astr. Ap.*, **107**, 292.
Schindler, M., Stencel, R. E., Linsky, J. L., Basri, G. S., and Helfand, D. J. 1982, *Ap. J.*, **263**, 269.
Simon, T. 1984, *Ap. J.*, **271**, 738.
Simon, T., Linsky, J. L., and Stencel, R. E. 1982, *Ap. J.*, **357**, 225.
Stencel, R. E., Linsky, J. L., Brown, A., Jordan, C., Carpenter, K. G., Wing, R. F., and Czyzak, S. 1981, *M.N.R.A.S.*, **196**, 47P.
Wilson, O. C. 1976, *Ap. J.*, **205**, 823.
Zirin, H. 1982, *Ap. J.*, **260**, 655.

A. BROWN: Joint Institute for Laboratory Astrophysics, University of Colorado, Boulder, CO 80309

A. K. DUPREE and L. HARTMANN: Center for Astrophysics, 60 Garden Street, Cambridge, MA 02138

C. JORDAN: University of Oxford, Department of Theoretical Physics, 1 Keble Road, Oxford OX1 3NP, England